Optical error budgeting using linearized ray-trace models

D. Redding
Jet Propulsion Laboratory, California Institute of Technology
4800 Oak Grove Drive, Pasadena CA 91109

ABSTRACT

The Root-Sum-Squared, or "RSS" wavefront error model is a simple, scalar tool, commonly used for space telescope error budgeting. At the same time, much more detailed models, combining ray-trace and Fourier optics with optical alignments and wavefront controls, can provide accurate, high-resolution simulations for detailed system and subsystem design. This paper makes a connection between the two modeling approaches by deriving RSS model coefficients from ray-trace models, including the effects of wavefront controls, for computing system performance from component error statistics. It is shown that, properly constructed, the simple RSS error budget is a covariance analysis, and can be as accurate as high-resolution wavefront models for statistical wavefront error prediction. A notional segmented-aperture space telescope is used to illustrate this error modeling process.

Keywords: Wavefront error, linearized ray-trace, wavefront control.

1. INTRODUCTION

One task of the optical system engineer is to manage the errors in the optical system – the figure and alignment errors of each optical element, for instance – to meet overall image quality requirements. These requirements can be written in terms of image-based metrics, such as Strehl ratio, encircled energy, or MTF. More commonly, the system Wavefront Error (WFE) is used as a surrogate for image quality, and the system engineer manages performance by budgeting the wavefront error contributions of all the various error sources to meet system-level WFE objectives. For a high-quality imaging telescope, the WFE will typically be specified so that the imagery will be limited by diffraction rather than aberrations, at a level of $1/10^{th}$ of a wavelength or better.

The Root-Sum-Squared, or "RSS" wavefront error model provides a simple and convenient scalar form for estimating total system WFE from the standard deviations of the various component errors, and is the most commonly used method for WFE budgeting:

$$WFE = \mathrm{sqrt}((coef_1 * \mathrm{std}(error_1))^2 + (coef_2 * \mathrm{std}(error_2))^2 + ...) \quad (1)$$

This paper uses high-dimensionality ray-trace methods to examine the RSS WFE model to determine its accuracy and scope. In particular, this paper:

1. Derives linearized ray-trace models for end-to-end performance, including active optical controls, such as rigid-body alignment actuators, or deformable mirrors.
2. Shows that RSS error models, properly formed, are covariance analyses.
3. Derives the WFE coefficients for component errors, and…
4. Illustrates the error modeling process for a notional large actively-controlled space telescope.

2. MODELING IMAGE FORMATION, IN A NUTSHELL

An imaging system, consisting of elements such as mirrors, lenses, apertures, filters, gratings, etc., plus a Focal Plane Array detector (FPA), takes in light emitted from a source, and brings it to a focus at the FPA. The source can be represented as a single point at the appropriate location, emitting rays of light in all directions simultaneously. Photons emitted at the same instant of time will lie upon a spherical surface located at the entrance pupil of the system, and centered at the source location. This spherical input reference surface is the ideal input wavefront of the system. Note that, for a source (such as a star) located very far away, this input wavefront surface is well represented as a plane.

The ideal output wavefront of the imaging system is similarly a sphere, located at the exit pupil of the system, and centered at the focal point on the FPA. The exit pupil is located at an image of the entrance pupil, established by the

optics between the entrance and exit of the system. For a typical telescope, the entrance pupil is the entrance aperture, and the exit pupil, conjugate to the aperture, is in virtual image space behind the secondary mirror.

Imperfections in the optical system, such as figure errors, misalignments, or "design error" – the design compromises that balance performance across the telescope field of view and spectral pass band – cause the actual wavefront to deviate from the ideal. This deviation, termed the Optical Path Difference (OPD), can be computed by tracing a grid of rays through the optical system, from the entrance pupil to the exit pupil. The ray-by-ray pathlength, minus the mean, can be plotted in a 2-dimensional map: an *OPD* matrix, showing how the pathlength varies across the pupil (Fig. 1).

The Wavefront Error (WFE) of the system is simply the RMS of those entries of the *OPD* matrix that fall within the system clear aperture.

The *OPD* map can also be used to calculate the Point Spread Function (*PSF*), which is the image of an unresolved source at the FPA. This is done using Fourier optics, by generating a complex amplitude (CA) matrix at the exit pupil by using the *OPD* and the wavelength (or wavelengths) to set the phase, and the ray transmission to set the magnitude, of each entry in the matrix. (Ray transmission is computed during the ray trace, based on element extent, extinction, polarization, and other properties.) The CA matrix at the FPA is then computed as the Fourier transform of the pupil amplitude matrix, plus a phase shift: Fraunhofer propagation[1]. The *PSF* is the modulus squared of the FPA CA matrix. By setting the sampling of the FPA CA matrix to correspond with the locations of the FPA pixels, the *PSF* can accurately simulate the image the real optical system would take of a star or other unresolved source (Fig. 1).

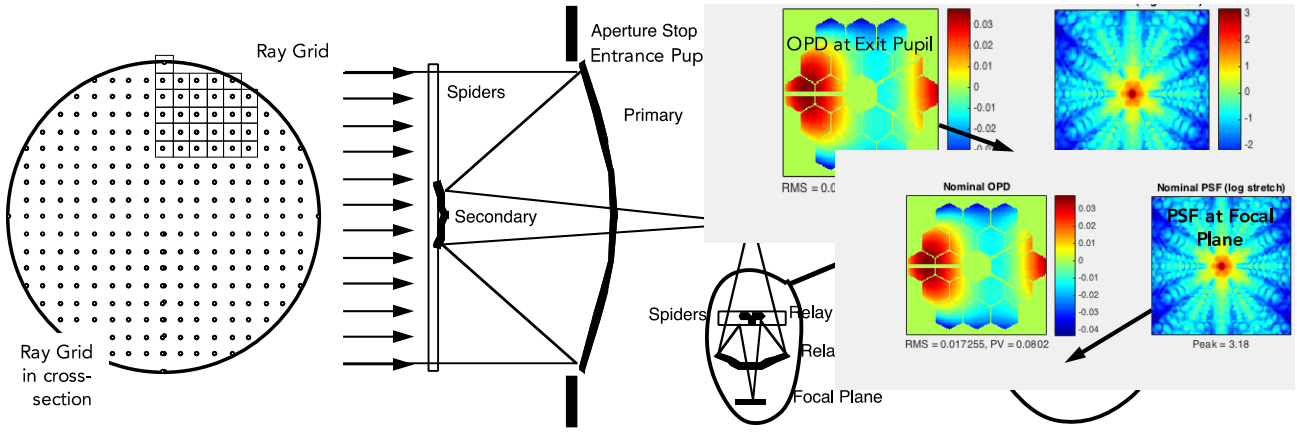

Figure 1. Elements used for ray-trace and Fourier optics modeling of a telescope.

3. LINEARIZED RAY-TRACE MODEL OF AN EXAMPLE TELESCOPE

To illustrate the points made in this paper we will use a notional space telescope design developed for the "ATLAST" study. Several ATLAST telescope concepts were developed to explore the scientific capabilities of a large UV-optical-NIR observatory, culminating in a white paper submitted to the 2010 Decadal Survey[2]. The design we will use here is for a large (8-16 meter) segmented-aperture space telescope, using a Three-Mirror Anastigmat (TMA) wide field design similar to that used for the James Webb Space Telescope (JWST). Like JWST, the Primary Mirror (PM) segments, and the Secondary Mirror (SM), are equipped with 6-DOF actuators, allowing them to be controlled on orbit. Unlike JWST, our example also includes a Deformable Mirror (DM) located at a pupil conjugate to the PM, and Figure Control Actuators on the PM segments. The DM and segment FCAs can also be controlled on orbit, to correct WF errors that may occur during fabrication, integration or launch. Our example system is sketched in Fig. 2.

The optical prescription of the example was entered into the JPL MACOS[3] optical modeling code, which was used to trace rays and generate PSFs for this analysis. MACOS implements the coordinate-free ray-trace theory of Refs. 4 and 5.

The OPD of the example can be computed by calls to MACOS (or any similar code), as:

$$OPD = \text{MACOS}(\textit{prescription data}, \textit{various commands}) \quad (1)$$

It is convenient to vectorize the OPD matrices we will be using. This is done as illustrated on Fig. 3, simply by stacking the column matrices of the OPD, excluding any entries that do not fall into the clear aperture.

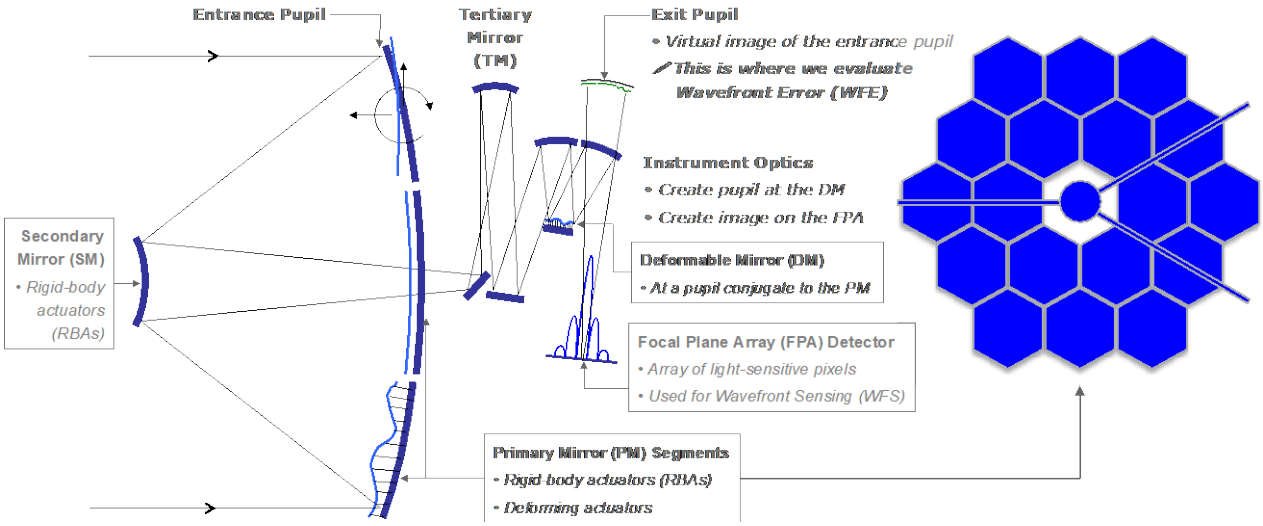

Figure 2. Example active telescope, showing key elements.

Thus:

$$w = \text{vector}(OPD) \tag{2}$$

and:

$$OPD = \text{matrix}(w) \tag{3}$$

The *WFE* is then:

$$WFE = \text{RMS}(w) = \text{RMS}(\text{nonzeros}(OPD)) \tag{4}$$

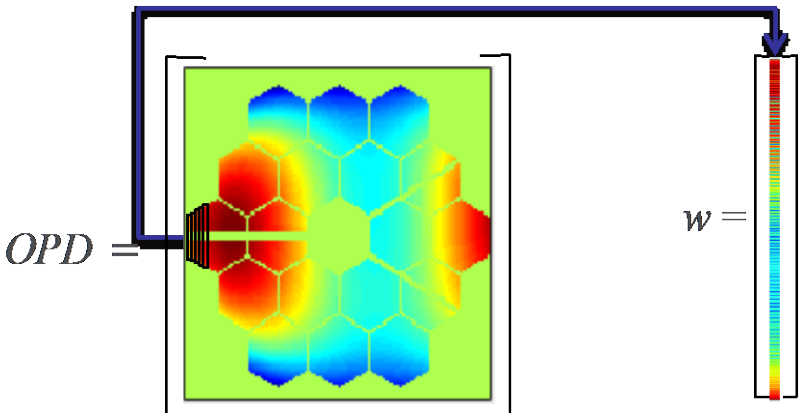

Figure 3. The OPD vector *w* is created by stacking column vectors from the *OPD* matrix.

The effect of perturbations of the optics, such as small motions of individual elements, or small changes in optical figure, can be computed by changing the optical prescription and recomputing the *OPD*. Figure 4 provides an example, showing the nominal *OPD*, the *OPD* after perturbing segment 2 with a small twist motion, and then showing the sensitivity of *w* to segment 2 twist. This sensitivity, denoted $\partial w/\partial x_{Poke}$, is computed as:

$$\frac{\partial w}{\partial Poke} = \frac{vector(OPD_{Poke} - OPD_0)}{\delta_{Poke}} \tag{5}$$

Here OPD_0 is the nominal OPD, and "δ_{Poke}" is the applied perturbation – in this case, applied to the twist degree of freedom (DOF) for segment 2. All the other pose DOFs can be treated in the same way, with the resulting column vectors organized into a single large sensitivity matrix, $\partial w/\partial x$. Here *x* is termed the optical state vector, and includes all of the rigid body (pose) DOFs. For the i^{th} optic, the pose state is:

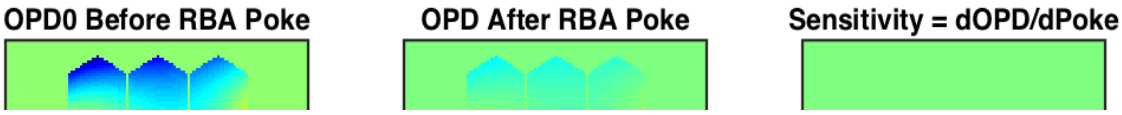

Figure 3. The sensitivity of w to twisting motion of segment 2: calculation by numerical differentiation.

$$\boldsymbol{x}_i = \begin{bmatrix} \theta \\ \delta \end{bmatrix} \tag{6}$$

where θ is a 3-vector of rotation and δ is a 3-vector of translation perturbations, usually in a local coordinate frame. The combined optical state x is:

$$\boldsymbol{x} = \begin{bmatrix} \boldsymbol{x}_1 \\ \square \\ \boldsymbol{x}_n \end{bmatrix} \tag{7}$$

Then the linearized ray-trace model of the OPD vector w that results from any combination of (small) pose changes is:

$$w = \frac{\partial w}{\partial x} x + w_0 \tag{8}$$

The dimension of the $\partial w / \partial x$ matrix is n_{ray} by n_{DOF}, with typically thousands of rays and hundreds of pose DOFs.

One can compute similar sensitivities for every other degree of freedom of interest in the optical prescription: for figure errors z; for PM segment and SM Rigid Body (RB) controls u_{RB}; for DM controls u_{DM}; and for PM segment figure control actuators u_{FCA}. Surface figure errors of each optic can be conveniently be represented using selected Zernike polynomials (Gram-Schmidt orthoganalized if not circularly shaped). For the ith optic in the example, the figure state is:

$$\boldsymbol{z}_i = \begin{bmatrix} Z_4 \\ \square \\ Z_{13} \end{bmatrix} \tag{9}$$

Here Z_i signifies the ith Zernike polynomial. The complete figure error state combines all optics as before:

$$\boldsymbol{z} = \begin{bmatrix} \boldsymbol{z}_1 \\ \square \\ \boldsymbol{z}_n \end{bmatrix} \tag{10}$$

The DM and FCA controls are organized similarly. The DM has 1313 actuators, so the DM control vector u_{DM} has dimension 1313x1. Each PM segment has 342 FCAs. For segment i:

$$u_{FCAi} = \begin{bmatrix} a_1 \\ \square \\ a_{342} \end{bmatrix} \tag{11}$$

For all optics:

$$u_{FCA} = \begin{bmatrix} u_{FCA1} \\ \vdots \\ u_{FCA18} \end{bmatrix} \tag{12}$$

Examples showing the OPD and PSF for selected pose and figure DOFs, and DM and FCA controls, are shown in Fig. 4.

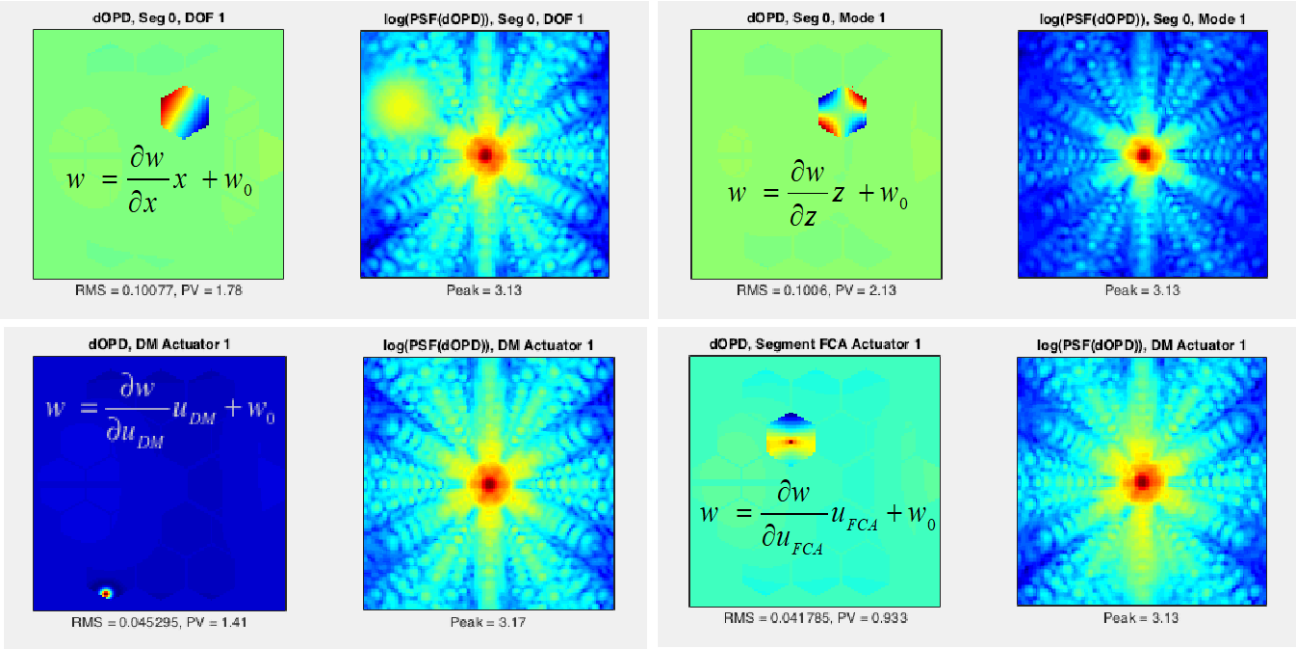

Figure 4. OPD and PSF for selected pokes: UL – effect of a local X-axis rotation of Segment 1; UR – Z4 applied to segment 1; LL – a DM actuator influence function; LR – a FCA influence function.

Combining all of these effects, the complete linearized ray-trace model of the OPD for the example system is:

$$w = \frac{\partial w}{\partial x} x + \frac{\partial w}{\partial z} z + \frac{\partial w}{\partial u_{RB}} u_{RB} + \frac{\partial w}{\partial u_{DM}} u_{DM} + \frac{\partial w}{\partial u_{FCA}} u_{FCA} + w_{nom} \tag{13}$$

4. WAVEFRONT CONTROL

Wavefront sensing and control (WFSC) uses measurements of the system to determine actuator settings that correct aberrations of the system. A thorough exposition of WFSC for telescopes like our example can be found in Ref. 6.

For the purposes of error modeling, it is not necessary to consider all of the steps that go into achieving the ultimate WFSC performance. Only the initial uncontrolled state (from Eq. 13), the final WFSC step, and any subsequent drift need be considered. In general, the final step will involve high resolution measurements of the WF followed by movement of the actuators, which then retain that position for some period of time – a month in the case of JWST. Uncompensated drifts are added to the final WFSC setting. Systems that include metrology or other additional measurements can provide useful control updates – these would compensate for drift effects. In our discussion here we

will discuss the final WFSC step only, and in an abbreviated form. Metrology-based control, assembly alignments, etc. can be handled in pretty much the same way.

WF control begins with WF sensing, a process by which the wavefront w can be estimated, as w_{est}. Examples of WF sensing methods include interferometric WF measurement, Shack-Hartmann or other WF slope measurement, and image-based phase retrieval[6]. In simplest form:

$$w_{est} = w + \delta w \tag{14}$$

Here δw is the noise in the measurement. In practice, the simple form of Eq. 14 should be replaced with a more detailed model representative of the actual methods used.

The control problem is to choose values for u that minimize the cost function:

$$J = 0.5\ (w - w_{nom})^{\mathrm{T}}(w - w_{nom}) \tag{15}$$

Subject to:

$$w_c = \frac{\partial w}{\partial u} du + w_{est} \tag{16}$$

$$u_{LB} \le u \le u_{UB}, \text{ where } u = u_0 + du \tag{17}$$

Here u stands for any or all of u_{RB}, u_{DM}, or u_{FCA}. Substituting w_c for w in Eq. 15, the solution comes at the stationary point $dJ = 0$:

$$dJ = 0 = du\left[\left(\frac{\partial w}{\partial u}\right)^T \frac{\partial w}{\partial u} u + \left(\frac{\partial w}{\partial u}\right)^T w_{est}\right] \tag{18}$$

The non-trivial solution:

$$u_1 = -G(w_{est} - w_{nom}) + \delta u \tag{19}$$

$$G = \left[\left(\frac{\partial w}{\partial u}\right)^T \frac{\partial w}{\partial u}\right]^{-1}\left(\frac{\partial w}{\partial u}\right)^T \equiv \left(\frac{\partial w}{\partial u}\right)^+ \tag{20}$$

This is the classic pseudo-inverse controller, easily implemented using constrained least-squares solvers such as Matlab's quadprog. The δu term is actuator noise.

5. END-TO-END WAVEFRONT PERFORMANCE SIMULATION

We now can simulate the complete wavefront performance of our example telescope. Again lumping the controls together, the OPD prior to control, as driven by initial misalignments and figure errors, is:

$$w_0 = \frac{\partial w}{\partial x} x_0 + \frac{\partial w}{\partial z} z_0 + \frac{\partial w}{\partial u} u_0 + w_{nom} \tag{21}$$

Specific values for the elements of x_0, z_0, and u_0 consistent with statistical design specifications can be realized using simple methods. For instance, a specification for initial alignment of the PM segments might require a 1-sigma error of 300 microns in each axis, based on achievable assembly tolerances and expected shifts during launch. Then a single realization of these errors can be computed using a normal-distribution random number generator, times the 300 microns standard deviation. Other distributions include uniform and worst-case, also handled in straightforward fashion.

Substituting for w_{est} and u_1 from Eqs. 14 and 19, the wavefront residual after WFSC is:

$$w_1 = P_u \frac{\partial w}{\partial x} x_0 + P_u \frac{\partial w}{\partial z} z_0 + \frac{\partial w}{\partial u} G \delta w_{est} + \frac{\partial w}{\partial u} \delta u \tag{22}$$

$$P_u = \left(I - \frac{\partial w}{\partial u} G\right) \tag{23}$$

Here the "control projection matrix" P_u will be zero only if the various actuators have full controllability of the OPD at the sampled ray density. This will not generally be true, and what leaks through – the imperfect correction residual – is known as fitting error. Other key terms are the sensing error – note that only the controllable part of the sensing error contributes to the post-control residuals – and the actuation error. Since actuator error levels are likely to be different between the RBAs, the DM and the FCAs, the overall impact of actuation error can be minimized through a control sequence that takes these differences into account.

The combined system WFE, post control, is the RMS of the OPD:

$$WFE_1 = \sqrt{\frac{1}{n}\left(\sum_j^{n_{ray}} w_{1_j}^2\right)} = \sqrt{\frac{w_1^T w_1}{n}} \tag{24}$$

This gives the WFE for a single realization of the various errors.

Given that the component specifications will be statistical, the overall WFE performance of the system will also be statistical, and no one realization will predict the likely performance of the as-built system. Many realizations, averaged, are required to do that. Monte Carlo analysis of the wavefront performance can be carried out by repeatedly generating initial errors x_0, z_0, and u_0 from their (statistical) specifications and computing the combined post-control WFE for each realization. Then the overall expected residual WFE performance is the average of all of the individual WFEs, with error bars determined from the scatter of the individual WFEs.

6. COVARIANCE ANALYSIS

There is another way to compute the expected system performance from statistical descriptions of the component errors, and that is by direct covariance analysis. The covariance of the end-to-end residual WFE w_1 is:

$$\mathrm{cov}(w_1) \equiv W_1 = \mathrm{E}(w_1 - \bar{w}_1)^T (w_1 - \bar{w}_1) \tag{25}$$

Substituting from Eq. 22:

$$W_1 = P_u \frac{\partial w}{\partial x} X_0 \frac{\partial w}{\partial x}^T P_u^T + P_u \frac{\partial w}{\partial z} Z_0 \frac{\partial w}{\partial z}^T P_u^T + \frac{\partial w}{\partial u} G W_{est} G^T \frac{\partial w}{\partial u}^T + \frac{\partial w}{\partial u} U \frac{\partial w}{\partial u}^T \tag{26}$$

Here the X_0, Z_0, U, and W_{est} signify the covariance matrices of x_0, z_0, δu, and δw_{est}, respectively. The expected value of the WFE, given these statistics and the linear model, is:

$$WFE = \sqrt{\frac{1}{n}\left(\sum_j^{n_{ray}} \sigma_{w_j}^2\right)} = \sqrt{\frac{1}{n}\mathrm{trace}(W)} \tag{27}$$

Many of the initial component errors will have the same statistics – zero mean, same standard deviation – and be uncorrelated. An example might be the initial placement of the PM segments. Assuming that similar but independent metrology is used in their initial placement, the initial misalignment of each segment would have the same (e.g., 300 micron) standard deviation, but each individual error is not related to any of the other errors. This would be the case, for instance, if the segments are installed within mechanical tolerances using laser tracker measurements.

In these cases the component errors with the same statistics can be grouped together for covariance analysis purposes. The initial covariance of that subset x_δ of the states that have placement error standard deviation σ_δ assumes a diagonal form:

$$X_\delta = \sigma_\delta^2 I \tag{28}$$

Plugging this into the W_1 equation, the contribution of segment misalignment to the total, post-control WFE is:

$$WFE_\delta = \sigma_\delta \alpha_\delta \tag{29}$$

This is a scalar equation, with a single coefficient α_δ multiplying the standard deviation σ_δ. The scalar coefficient, however, is computed from the product of very large matrices, which embed the full linearized optical model, including the effect of the WFSC controls:

$$\alpha_\delta = \sqrt{\frac{1}{n}\text{trace}\left(P_u \frac{\partial w}{\partial x_\delta} \frac{\partial w}{\partial x_\delta}^T P_u^T \right)} \tag{30}$$

This approach can be carried out for all of the errors and noises in the linearize ray-trace model. For instance, the WFE due to DM actuator error is:

$$WFE_{u_{DM}} = \sigma_{u_{DM}} \alpha_{u_{DM}}, \text{ where: } \alpha_{u_{DM}} = \sqrt{\frac{1}{n}\text{trace}\left(\frac{\partial w}{\partial u_{DM}} \frac{\partial w}{\partial u_{DM}}^T \right)} \tag{31}$$

Similarly the effect of estimation error can be written:

$$WFE_{w_{est}} = \sigma_{w_{est}} \alpha_{w_{est}}, \text{ where: } \alpha_{w_{est}} = \sqrt{\frac{1}{n}\text{trace}\left(\frac{\partial w}{\partial u} G G^T \frac{\partial w}{\partial u}^T \right)} \tag{32}$$

These terms can be combined using root-sum-square to calculate the expected WFE due to all of the component errors:

$$WFE = \sqrt{\sigma_{x_{0_{wfg}}}^2 \alpha_{x_{0_{wfg}}}^2 + \cdots + \sigma_{z_{4_{wfg}}}^2 \alpha_{x_{4_{wfg}}}^2 + \cdots + \sigma_{w_{est}}^2 \alpha_{w_{est}}^2 + \cdots + \sigma_{u_{RB_{wfg}}}^2 \alpha_{u_{RB_{wfg}}}^2 + \cdots} \tag{33}$$

Thus we have re-derived Eq. 1, the classic RSS-form error model commonly used for error budgeting.

By computing the coefficients following the approach here, the RSS model becomes a covariance analysis. As such, it is subject to certain limitations. In particular, it is assumed that the system is indeed linear, and that the sensitivities are accurate. This will be true for a well-designed system operating near its design condition. Second, the component errors in this derivation are implicitly assumed zero-mean and normally distributed. In practice, non-normally distributed errors are important.

Equation 33 can be implemented in a spreadsheet form, as indicated in Fig. 5, which also rolls up the performance of our example system. In this spreadsheet, the white cells contain the input component error σ's. The other cells are linked to the α coefficients on another worksheet, for pre- and post-WFSC wavefront error. The effect of each term, as well as the sum of all terms, are shown in the corresponding cells. This form allows the system engineer to rapidly change error distributions, accurately assessing the system WFE consequences of changes made to source-level error specifications, without having to run large simulations.

The ATLAST segmented aperture telescope notional design used to illustrate the points made here was used to explore the performance requirements for a large-aperture telescope for astronomy prior to the 2010. As shown in Fig. 5, WFSC was shown to help reduce large initial errors to values consistent with an overall WFE budget of 20 nm. As NASA nears the 2020 Decadal Survey, LUVOIR, a large UV/optical/IR telescope concept, generally following the characteristics identified in recent studies[7] has been selected as one of four studies for funded study leading to consideration for mission start in the decade of the 2020s.

7. COVARIANCE VS. MONTE CARLO ANALYSIS

Monte Carlo analysis can also be used to compute the coefficients α, by exercising Eqs. 22 and 24 (etc.) many times with only particular component errors included, isolating each individual error term, and using the average WFE response to determine the coefficient for that term. This can be done without assuming normal distribution for the error statistics. It can embed non-linear effects, such as sensor or actuator discretization, or nonlinear optics or controls. This approach can also be computationally more efficient than directly evaluating the covariance analysis coefficients, especially for highly correlated errors (such as PSD-based figure specifications).

When the assumptions are the same between covariance analysis and Monte Carlo analysis, the results will also be the same. This is illustrated in Fig. 5, which overlays RSS-model and full Monte Carlo results (with many trials) for a case like our example, but with only 4 DOF control for the mirror segments. As shown, the results are indeed the same

between the simple RSS model and the big elaborate Monte Carlo analysis. The performance error floor is set by design error in these examples.

9/1/08	Segmented Telescope WFE Budget	Initial Alignment			Metrology Control				Total WFE
	Degree of Freedom	Inputs		RMS WFE (nm)		Drift Inputs		RMS WFE (nm)		Post Metrology
		Values	Units	Pre WFC	Post WFC	Values	Units	Pre Metrology	Post Metrology	RMS WFE (nm)
Optical Telescope Assembly	PM Segment Tilt	2,000	urad	1,715,156	0.0	50	urad	42,879	0.0	0.0
	PM Segment Piston	1,000,000	nm	1,819,286	0.0	1,000	nm	1,819	0.0	0.0
	PM Segment Decenter	1,000,000	nm	47,080	0.3	1,000	nm	47	0.0	0.3
	PM Segment Clocking	3,000	urad	336	0.8	15	urad	2	0.9	1.2
	PM Low-order Figure (0-5 cycles/seg	300	nm	578	5.9	2	nm	4	3.9	7.0
	PM PSD Figure	6	nm	11	5.5	1	nm	1.8	1.8	5.8
		0.003	c/mm			0.003	c/mm			
	PM Segment Mandrels	408	nm	816	6.0					6.0
	PM Print Through	1,000	Pa	18	1.2					1.2
	PM Thermal	18.0	deg C	1,904	2.9	0.020	deg C	2	2.1	3.6
	PM Nanolaminate Strain	26	deg C	2,218	3.9	0.000	deg C	0	0.0	3.9
	SM Decenter	2,000,000	nm	258,751	0.0	2,500	nm	323	0.0	0.0
	SM Piston	2,000,000	nm	2,620,916	0.0	2,000	nm	2,621	0.0	0.0
	SM Clocking	2,500	urad	0	0.0	2,000	urad	0	0.0	0.0
	SM Tilt	5,000	urad	1,337,236	0.0	120	urad	32,094	0.0	0.0
	SM Low-Order Figure	30	nm	38	0.2	1	nm	1	1.3	1.3
	SM PSD Figure	15	nm	35	2.9	1	nm	1	1.4	3.2
		0.003	c/mm			0.003	c/mm			
				●	●	●				
WFC	WFS Error	3	nm	13	2.4		nm			2.4
	PM RB Actuator Error	2	nm	0	1.6		nm	0	0.0	1.6
	PM DM Actuator Error	2	V	0	0.0		units	0	0.0	0.0
	SM RB Actuator Error									
	PM thermal ΔT	0.000	°C	0	0.0	0.100	°C	7	6.0	6.0
WFE Summary	PM WFE			2,500,757	11.2			42,918	4.9	12.2
	Everything Else			2,953,737	7.3			32,218	8.9	11.5
	Design WFE	10	nm		10.0					10.0
	Payload WFE									19.5
	WFE Requirement									20.0
	WFE Margin									2.3%

Figure 5. Spreadsheet excerpt for the RSS error model of the example system.

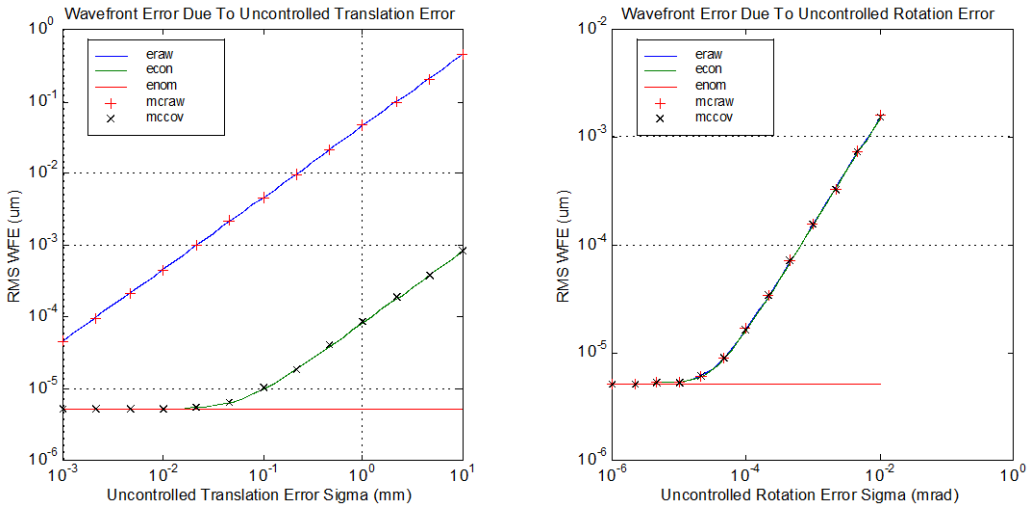

Figure 6. WFE computed using RSS covariance analysis (solid lines) compared to WFE computed from Monte Carlo methods (points), showing good agreement.

8. CONCLUSION

The RSS error budget is a simple and useful tool. Properly constructed, it can be as accurate as much larger and more complex models, even for actively controlled optical systems, such as segmented-aperture space telescopes.

9. ACKNOWLEDGEMENTS

Thanks to Scott Basinger and Philip Dumont for their contributions. This work was performed at the Jet Propulsion Laboratory, California Institute of Technology, under contract with NASA.

REFERENCES

[1] Goodman, J., [Introduction to Fourier Optics], McGraw-Hill, New York, 1968.

[2] Postman, M. and 67 others, "Advanced Technology Large Aperture Space Telescope (ATLAST): A Technology Roadmap for the Next Decade," white paper submitted to the NRC ASTRO-2010 Survey (2009).

[3] [MACOS Manual], JPL document.

[4] Redding, D. and Breckenridge W., "Optical Modeling for Dynamics and Control Analysis," Journal of Guidance, Control and Dynamics, September 1991.

[5] Redding, D. and Breckenridge W., "Linearized Ray-Trace Analysis," SPIE 1354 (1990). Also in [Selected SPIE Papers on CD ROM, Volume 2, Lens Design], D. O'Shea, ed., 1998.

[6] Redding, D., Shi, F., Basinger, S., Cohen, D., Green, J., Lowman, A. and Ohara, C., "Wavefront Control for Large Space Optics," IEEE Aerospace Conference (2003).

[7] Dalcanton, J., Seager, S., Aigrain, S., Battel, S., Brandt, D., Conroy, C., Feinberg, L., Gezari, S., Guyon, O., Harris, W., Hirata, C., Mather, J., Postman, M., Redding, D., Schiminovich, D., Stahl, H. [From Cosmic Birth to Living Earths], http://www.hdstvision.org, AURA (2015).